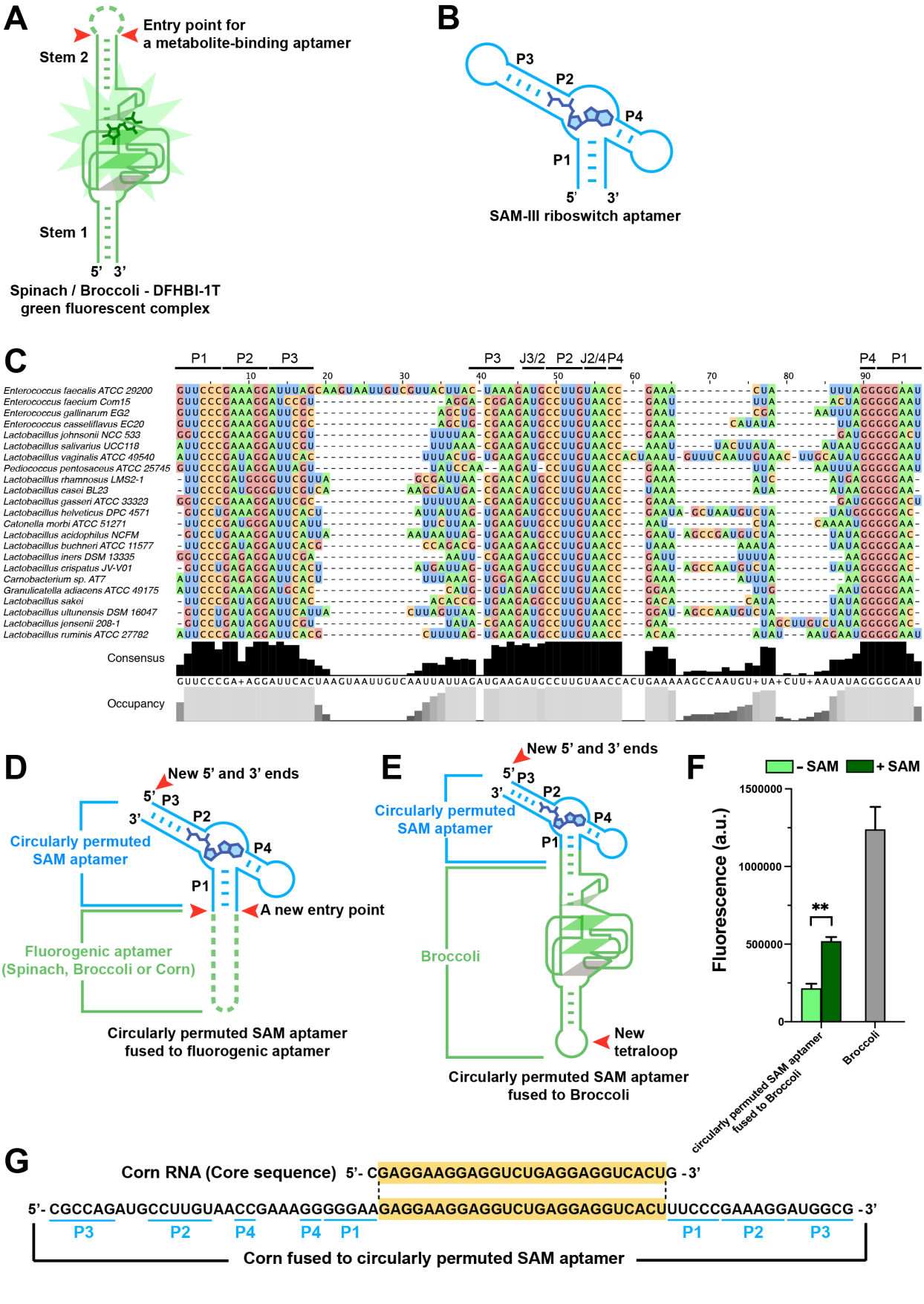
A
Entry point for
a metabolite-binding aptamer
Stem 2
Stem 1
5' 3'
Spinach / Broccoli - DFHBI-1T
green fluorescent complex
B
P3
P2
P4
P1
5' 3'
SAM-III riboswitch aptamer
C
P1 P2 P3 P3 J3/2 P2 J2/4 P4 P4 P1
Enterococcus faecalis ATCC 29200
Enterococcus faecium Com15
Enterococcus gallinarum EG2
Enterococcus casseliflavus EC20
Lactobacillus johnsonii NCC 533
Lactobacillus salivarius UCC118
Lactobacillus vaginalis ATCC 49540
Pediococcus pentosaceus ATCC 25745
Lactobacillus rhamnosus LMS2-1
Lactobacillus casei BL23
Lactobacillus gasseri ATCC 33323
Lactobacillus helveticus DPC 4571
Catonella morbi ATCC 51271
Lactobacillus acidophilus NCFM
Lactobacillus buchneri ATCC 11577
Lactobacillus iners DSM 13335
Lactobacillus crispatus JV-V01
Carnobacterium sp. AT7
Granulicatella adiacens ATCC 49175
Lactobacillus sakei
Lactobacillus ultunensis DSM 16047
Lactobacillus jensenii 208-1
Lactobacillus ruminis ATCC 27782
Consensus
Occupancy
D
New 5' and 3' ends
5' P3
3'
P2
P4
P1
Circularly permuted
SAM aptamer
A new entry point
Fluorogenic aptamer
(Spinach, Broccoli or Corn)
Circularly permuted SAM aptamer
fused to fluorogenic aptamer
E
New 5' and 3' ends
5' P3
3'
P2
P4
P1
Circularly permuted
SAM aptamer
Broccoli
New
tetraloop
Circularly permuted SAM aptamer
fused to Broccoli
F
- SAM
+ SAM
Fluorescence (a.u.)
1500000
1000000
500000
0
**
circularly permuted SAM aptamer
fused to Broccoli
Broccoli
G
Corn RNA (Core sequence) 5'- CGAGGAAGGAGGUCUGAGGAGGUCACUG -3'
5'- CGCCAGAUGCCUUGUAACCGAAAGGGGGAAGAGGAAGGAGGUCUGAGGAGGUCACUUUCCCGAAAGGAUGGCG -3'
P3 P2 P4 P4 P1 P1 P2 P3
Corn fused to circularly permuted SAM aptamer

Figure S1, related to Figure 1. Circularly permuted SAM aptamer creates an entry point for a fluorogenic aptamer

(A) Schematic representation of the Spinach structure shows an entry point for a metabolite binding aptamer. Spinach contains two helical stems (Stem 1 and Stem 2, indicated). The cognate fluorophore DFHBI-1T (Song et al., 2014) binds between the top G-quadruplex (green parallelogram) and a base-triple (grey triangle). Stem 2 above the base triple provides an entry point for metabolite-binding aptamers, which have been used to generate Spinach-based metabolite sensors. The principles shown here also apply to the Broccoli aptamer, which has a very similar fluorophore-binding domain (Filonov et al., 2019). The transparent grey parallelogram indicates a mixed-sequence tetrad.

(B) Schematic representation of the SAM-III riboswitch aptamer structure in complex with SAM (Lu et al., 2008).

(C) Phylogenetic sequence alignment of the SAM-III riboswitch aptamer RNA (Appasamy et al., 2013; Fuchs et al., 2006). The sequences of the P3 stem adjacent to the loop region do not show high conservation across different prokaryotic cell species.

(D) Schematic diagram of circularly permuted SAM aptamer fused to a fluorogenic aptamer. Circularly permuted SAM aptamer contains new 5' and 3' ends at the end of P3 stem, instead of the P1 stem. This creates a new entry point in the P1 stem for inserting a fluorogenic aptamer such as Spinach, Broccoli or Corn.

(E) To test whether the circularly permuted SAM aptamer is functional, we fused this newly engineered SAM aptamer to Broccoli. The schematic diagram shows that the P1 stem of the circularly permuted SAM aptamer fused to the Broccoli stem. Also shown are the 5' and 3' ends introduced into the P3 stem of the circularly permuted SAM aptamer.

(F) Fluorescence measurements for the circularly permuted SAM aptamer-Broccoli fusion RNA in the absence or presence of SAM. The fluorescence signal of 1 μM *in vitro* transcribed fusion RNA was measured at 37°C after the addition of vehicle (water) or 0.1 mM SAM in buffer containing 40 mM K-HEPES (pH 7.5), 100 mM KCl, 1 mM $MgCl_2$ and 10 μM DFHBI-1T. (excitation 470 nm; emission 505 nm). The mean and SEM values are shown (n = 3). ** P = 0.0021

(G) The core sequence of Corn and the sequence of Corn fused to the circularly permuted SAM aptamer. Each helical stem of the SAM aptamer is denoted on the sequence of the fusion RNA (below).

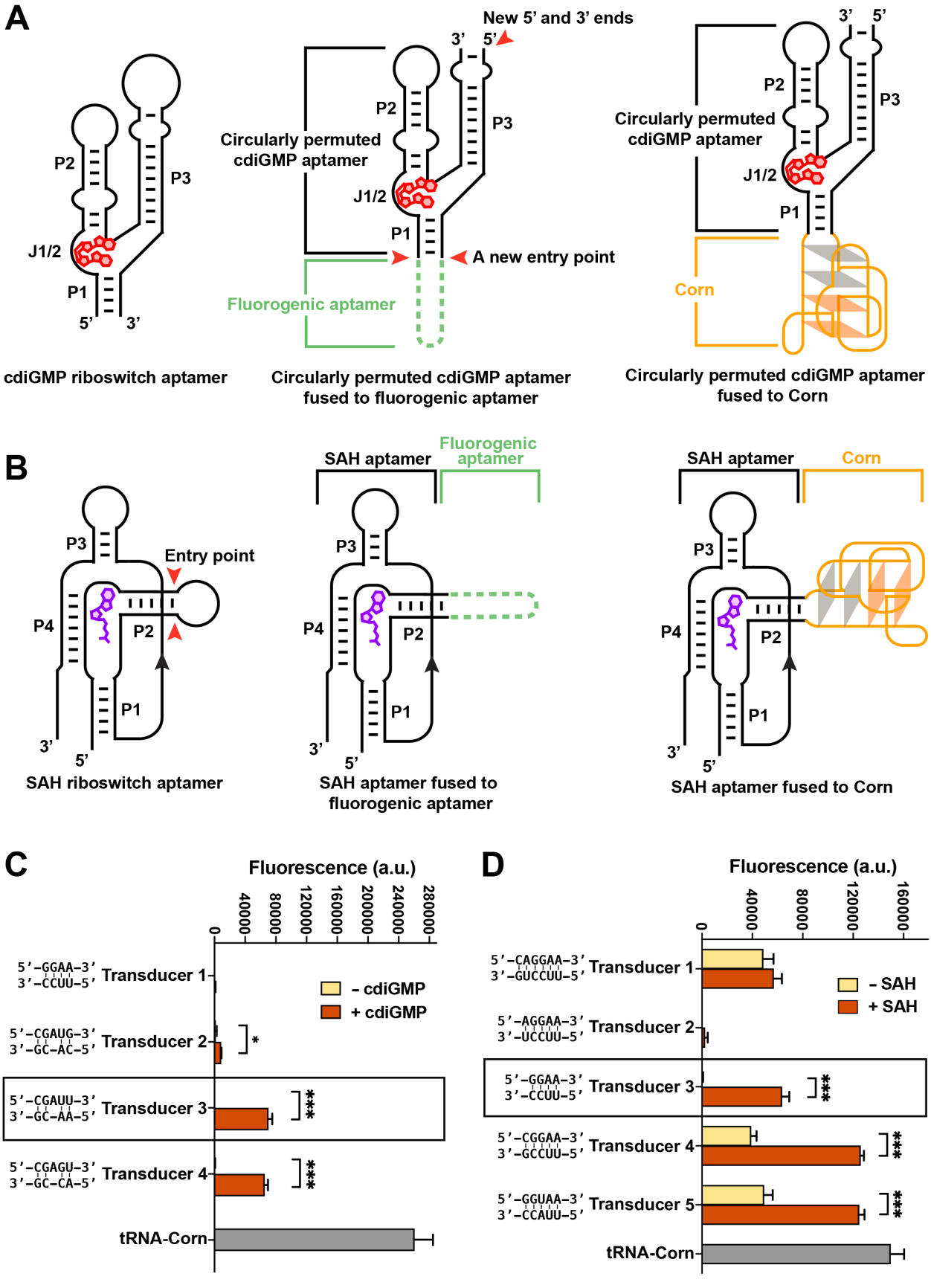
A
P2
P3
J1/2
P1
5'
3'
cdiGMP riboswitch aptamer
New 5' and 3' ends
3'
5'
P2
P3
Circularly permuted
cdiGMP aptamer
J1/2
P1
A new entry point
Fluorogenic aptamer
Circularly permuted cdiGMP aptamer
fused to fluorogenic aptamer
3'
5'
P2
P3
Circularly permuted
cdiGMP aptamer
J1/2
P1
Corn
Circularly permuted cdiGMP aptamer
fused to Corn
B
P3
Entry point
P4
P2
P1
3'
5'
SAH riboswitch aptamer
SAH aptamer
Fluorogenic
aptamer
P3
P4
P2
P1
3'
5'
SAH aptamer fused to
fluorogenic aptamer
SAH aptamer
Corn
P3
P4
P2
P1
3'
5'
SAH aptamer fused to Corn
C
Fluorescence (a.u.)
0
40000
80000
120000
160000
200000
240000
280000
5'-GGAA-3'
3'-CCUU-5'
Transducer 1
5'-CGAUG-3'
3'-GC-AC-5'
Transducer 2
*
5'-CGAUU-3'
3'-GC-AA-5'
Transducer 3
***
5'-CGAGU-3'
3'-GC-CA-5'
Transducer 4
***
tRNA-Corn
- cdiGMP
+ cdiGMP
D
Fluorescence (a.u.)
0
40000
80000
120000
160000
5'-CAGGAA-3'
3'-GUCCUU-5'
Transducer 1
5'-AGGAA-3'
3'-UCCUU-5'
Transducer 2
5'-GGAA-3'
3'-CCUU-5'
Transducer 3
**
5'-CGGAA-3'
3'-GCCUU-5'
Transducer 4
***
5'-GGUAA-3'
3'-CCAUU-5'
Transducer 5
***
tRNA-Corn
- SAH
+ SAH

Figure S2, related to Figure 2. Design of a Corn-cdiGMP sensor and a Corn-SAH sensor.

(A) Schematic diagram of designing a Corn-cdiGMP sensor. Circularly permuted cdiGMP aptamer contains new 5' and 3' ends at the end of the P3 stem, instead of the P1 stem. This creates a new entry point in the P1 stem for inserting a fluorogenic aptamer such as Spinach, Broccoli or Corn. We fused this newly engineered cdiGMP aptamer to Corn.

(B) Schematic diagram of a Corn-SAH sensor. The SAH aptamer contains an entry point in the P2 stem for inserting a fluorogenic aptamer such as Spinach, Broccoli or Corn. Thus, Corn was fused to the P2 stem on the SAH aptamer.

(C) Optimization of cdiGMP-Corn sensor transducer sequences. Four different transducer sequences were tested for their ability to mediate cdiGMP-induced fluorescence. In each case, *in vitro* transcribed Corn-SAM sensor RNA (1 μM) was incubated with 10 μM DFHO and 0.1 mM cdiGMP in buffer containing 40 mM K-HEPES (pH 7.5), 100 mM KCl and 3 mM $MgCl_2$. After 1 h incubation at 37°C, the fluorescence of each sample was measured (excitation 505 nm; emission 545 nm). The optimal transducer (transducer 3), based on signal-to-noise ratio, is indicated in a black-lined box. The mean and SEM values are shown in the plot (n = 3). * P = 0.0116 (Transducer 2), *** P = 0.0002 (Transducer 3), *** P = 0.0001 (Transducer 4)

(D) Optimization of SAH-Corn sensor transducer sequences. Five different transducer sequences were tested for their ability to mediate SAH-induced fluorescence. In each case, *in vitro* transcribed Corn-SAM sensor RNA (1 μM) was incubated with 10 μM DFHO and 0.1 mM SAH in buffer containing 40 mM K-HEPES (pH 7.5), 100 mM KCl and 0.5 mM $MgCl_2$. After 1 h incubation at 37°C, the fluorescence of each sample was measured (excitation 505 nm; emission 545 nm). The optimal transducer (transducer 3), based on signal-to-noise ratio, is indicated in a black-lined box. The mean and SEM values are shown in the plot (n = 3). *** P = 0.0004 (Transducer 3), *** P < 0.0001 (Transducer 4), *** P = 0.0008 (Transducer 5)

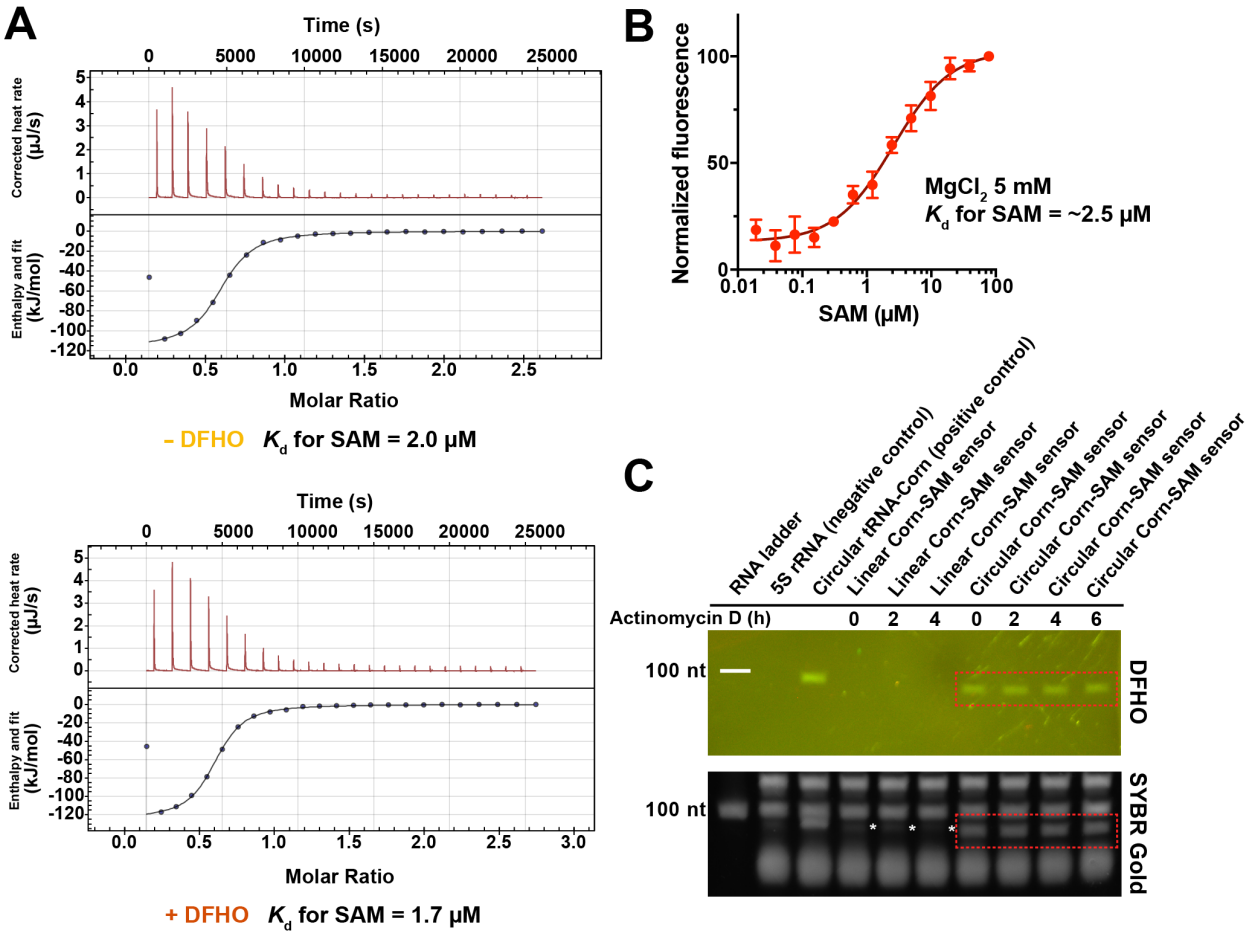
A
Time (s)
Corrected heat rate (μJ/s)
Enthalpy and fit (kJ/mol)
Molar Ratio
- DFHO K_d for SAM = 2.0 μM
+ DFHO K_d for SAM = 1.7 μM
B
Normalized fluorescence
SAM (μM)
$MgCl_2$ 5 mM
K_d for SAM = ~2.5 μM
C
RNA ladder
5S rRNA (negative control)
Circular tRNA-Corn (positive control)
Linear Corn-SAM sensor
Circular Corn-SAM sensor
Actinomycin D (h)
100 nt
DFHO
SYBR Gold
D
Normalized absorbance
No transfection
5S rRNA
Circular tRNA-Corn
Circular Corn-SAM sensor
Linear Corn-SAM sensor
E
Continuous illumination
Normalized fluorescence
Circular Corn sensor
Circular Broccoli sensor
Time (s)
F
Circular Corn sensor
Circular Broccoli sensor
Recovery interval (s)

Figure S3, related to Figures 3 and 4. Circular Corn-SAM sensor expressed using the Tornado system accumulates to high concentration level in HEK293T cells and exhibits markedly improved photostability.

(A) ITC measurements for the K_d of the Corn-SAM sensor for SAM in the presence or absence of DFHO. We measured SAM binding to the Corn-SAM sensor using a previous protocol used to study DFHO binding to Corn (Song et al., 2017). In these experiments, Corn-SAM sensor RNA solution and SAM solution were prepared in the same buffer (40 mM K-HEPES, pH 7.5, 100 mM KCl and 5 mM $MgCl_2$). In ITC experiments, RNA is used at a high concentration, which required us to similarly increase the concentration of DFHO and $MgCl_2$ in order to maintain stoichiometry with respect to the RNA. *In vitro* transcribed Corn-SAM sensor was dissolved to a final concentration ~107.5 µM in a 330 µL solution. In the condition where DFHO was present, 400 µM DFHO was included in the final RNA solution (final concentration of DMSO was 0.56%). The RNA solution was loaded in the cell of a Nano ITC microcalorimetry device (TA Instruments) and 50 µL of 877 µM SAM was loaded in the titration syringe. For the condition where DFHO was present, 0.56% DMSO was included in the final SAM solution. Measurements were performed at 37°C and the syringe rotation speed was set to 250 rpm. Data were fit with using the "independent model" setting in NanoAnalyze software (TA Instruments). The concentration of Corn-SAM sensor RNA was determined using denaturing PAGE analysis followed by SYBR Gold staining and comparing SYBR Gold signal with RNA standards (Thermo Fisher Scientific SM1831).

(B) Dose-response curve for fluorescence activation of the Corn-SAM sensor by SAM. In the ITC experiment, more $MgCl_2$ is used due to the high concentration of RNA. We therefore measured the SAM EC_{50} using high (i.e. 5 mM) $MgCl_2$ conditions for comparison with the ITC results shown in panel A. For these experiments, *in vitro* transcribed Corn-SAM sensor RNA (0.1 µM) was incubated with each indicated concentration of SAM and 10 µM DFHO at 37°C in a buffer containing 40 mM K-HEPES (pH 7.5), 100 mM KCl and 5 mM $MgCl_2$. Half-maximal fluorescence is reached at ~2.5 µM. This value is comparable to the K_d value obtained from ITC shown in panel A. The Hill coefficient calculated using GraphPad Prism was ~1. The mean and SEM values are shown (n = 3).

(C) Denaturing PAGE analysis of whole cellular RNA harvested from cells expressing different RNA constructs. To confirm expression of the circular Corn-SAM sensor and its long half-life, we harvested total cellular RNA from cells treated with actinomycin D for the indicated time and analyzed the RNA by denaturing PAGE. HEK293T cells were transfected with a plasmid expressing the linear Corn-SAM sensor or a plasmid expressing the circular Corn-SAM sensor. 2 d after transfection, cells were treated with 5 µg/ml actinomycin D for the indicated time to inhibit RNA polymerase activity, and thus measure RNA stability. Total cellular RNA was harvested by using TRIzol LS. Cellular RNA (1.5 µg) was loaded in each lane of a 6% TBE-Urea PAGE gel. After PAGE, the gel was washed three times for 5 min each with water to remove urea from the gel. Then, the gel was first stained with 10 µM DFHO and 0.1 mM SAM (top), followed by a counterstaining with SYBR Gold (bottom). The DFHO stained gel was imaged using a ChemiDoc Imaging station (BioRad) at the green channel (excitation 470/30 nm; emission 530/28 nm) and red channel (excitation 530/28 nm; emission 605/50 nm). The image shown here is the overlay of both scans. The SYBR Gold stained gel was imaged using standard imaging settings (excitation 302 nm; emission 590/110 nm).

Red dotted boxes indicate circular Corn-SAM sensor RNA. Unlike the circular form of the sensor, which was readily detected on the DFHO-stained denaturing PAGE gel, the linear form

of the sensor was not detected. Notably, treatment of cells with actinomycin D for 6 h, which typically causes a complete loss of linear aptamers due to their instability, did not affect the expression level of the circular Corn-based sensor. This is expected for circular RNA. White asterisks on the SYBR Gold stained gel indicate the faint linear Corn-SAM sensor RNA.

(D) Cells were assayed for viability and proliferation with MTT. Cells were transfected with plasmids expressing the indicated RNA constructs. Cells were subcultured onto mouse laminin-coated plates 1 d after transfection. 3 d after transfection, cells were incubated with 2.5 mg/mL MTT. After 3 h incubation at 37°C, cells were lysed. MTT absorbance readings were performed at 590 nm absorbance. Signal obtained from MTT solution without cells was used for subtracting background. Values were normalized to the average value of the no transfection condition.

(E) Photostability analysis of the circular Corn-SAM sensor and the circular Broccoli-SAM sensor with continuous illumination. In **Figures 4, S3F and S4**, we used pulsed illumination, which reduces photobleaching. Here we used a continuous illumination protocol. To test if the Corn-SAM sensor exhibits improved photostability compared to the Broccoli-SAM sensor, we imaged cells expressing the circular Corn-SAM sensor or the circular Broccoli-SAM sensor (Litke and Jaffrey, 2019). Cell images were acquired for 10 s using a 400 ms acquisition time. The cells were continuously illuminated throughout the experiment. Cellular mean fluorescence intensity was calculated (See **Methods**), and normalized to maximum intensity at time point 400 ms (100) and background intensity (0). The normalized values of cell mean fluorescence intensity were plotted against time. The average values of mean fluorescence intensity and SEM calculated from cells in independently acquired images are shown on the plot (n = 3). Representative images are shown. The filter set used for Broccoli fluorescence detection was a filter cube with excitation filter 470 ± 20 nm, dichroic mirror 495 nm (long pass), and emission filter 525 ± 25 nm. Corn fluorescence detection used a filter cube with excitation filter 500 ± 12 nm, dichroic mirror 520 nm (long pass), and emission filter 542 ± 13.5 nm. Scale bar 10 μm. NA 0.75.

(F) Photostability analysis of the circular Corn-SAM sensor and the circular Broccoli-SAM sensor with pulsed illumination. We examined if fluorescence intensity in single cells expressing the Corn-SAM sensor or the Broccoli-SAM sensor photobleaches during the short time-course imaging experiment. Cell images were acquired with a 1000-ms acquisition time. A recovery interval (i.e. shutter closed, and no light was applied to samples) was either 10 s or 5 s, as indicated. The fluorescence intensity in cells expressing the Broccoli-SAM sensor exhibited substantially more photobleaching compared to Corn-SAM sensor expressing cells (See **Figure 4B**). Scale bar 10 μm. NA 0.75.

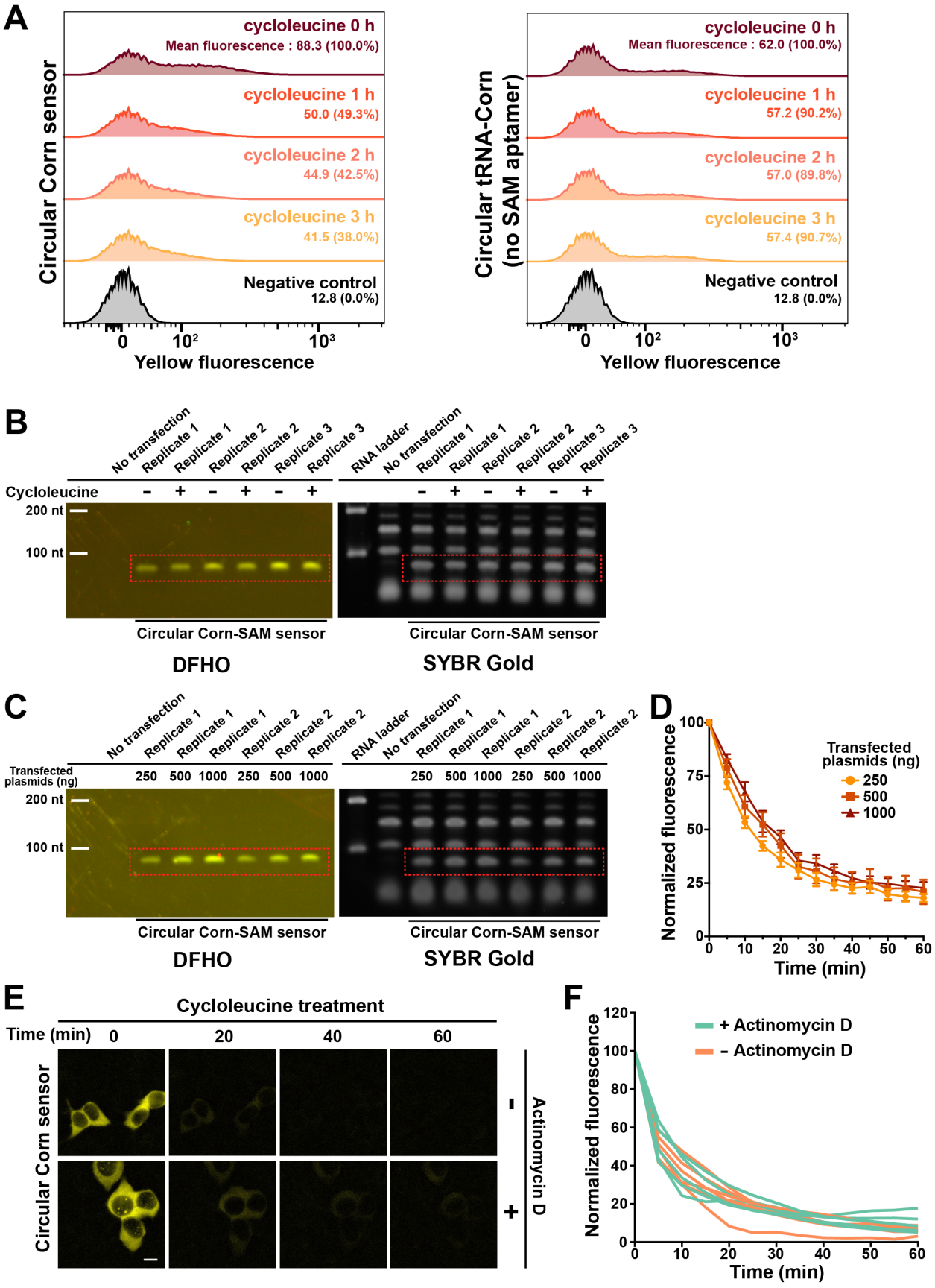
A
Circular Corn sensor
cycloleucine 0 h
Mean fluorescence : 88.3 (100.0%)
cycloleucine 1 h
50.0 (49.3%)
cycloleucine 2 h
44.9 (42.5%)
cycloleucine 3 h
41.5 (38.0%)
Negative control
12.8 (0.0%)
0
10²
10³
Yellow fluorescence
Circular tRNA-Corn (no SAM aptamer)
cycloleucine 0 h
Mean fluorescence : 62.0 (100.0%)
cycloleucine 1 h
57.2 (90.2%)
cycloleucine 2 h
57.0 (89.8%)
cycloleucine 3 h
57.4 (90.7%)
Negative control
12.8 (0.0%)
0
10²
10³
Yellow fluorescence
B
No transfection
Replicate 1
Replicate 1
Replicate 2
Replicate 2
Replicate 3
Replicate 3
RNA ladder
No transfection
Replicate 1
Replicate 1
Replicate 2
Replicate 2
Replicate 3
Replicate 3
Cycloleucine
- + - + - +
- + - + - +
200 nt
100 nt
Circular Corn-SAM sensor
Circular Corn-SAM sensor
DFHO
SYBR Gold
C
No transfection
Replicate 1
Replicate 1
Replicate 1
Replicate 2
Replicate 2
Replicate 2
RNA ladder
No transfection
Replicate 1
Replicate 1
Replicate 1
Replicate 2
Replicate 2
Replicate 2
Transfected plasmids (ng)
250 500 1000 250 500 1000
250 500 1000 250 500 1000
200 nt
100 nt
Circular Corn-SAM sensor
Circular Corn-SAM sensor
DFHO
SYBR Gold
D
Normalized fluorescence
100
75
50
25
0
0 10 20 30 40 50 60
Time (min)
Transfected plasmids (ng)
250
500
1000
E
Cycloleucine treatment
Time (min) 0 20 40 60
Circular Corn sensor
-
+
Actinomycin D
F
Normalized fluorescence
120
100
80
60
40
20
0
0 10 20 30 40 50 60
Time (min)
+ Actinomycin D
- Actinomycin D

Figure S4, related to Figure 4. Changes in Corn fluorescence reflect SAM dynamics in living cells.

(A) Flow cytometry analysis of cells expressing the circular Corn-SAM sensor after cycloleucine treatment, which inhibits SAM biosynthesis. HEK293T cells were transfected with plasmids expressing the circular Corn-SAM sensor. As a control for the cycloleucine response, cells expressing the circular tRNA-Corn were analyzed. Cells were subcultured onto mouse laminin-coated plates 1 d after transfection. 2 d after transfection, we treated cells with 25 mM cycloleucine for the indicated time. Yellow fluorescence was collected (excitation 488 nm; emission 545 ± 17.5 nm). Cells expressing 5S rRNA were used to establish cellular autofluorescence. Both U6 promoter for the circular Corn-based constructs transcription and 5S promoter for 5S rRNA transcription recruit RNA polymerase III (White, 2004). The number of cells were plotted as a histogram against the yellow fluorescence signal intensity. Mean fluorescence values are shown.

(B) Denaturing PAGE analysis of whole cellular RNA harvested from cells treated with cycloleucine and control cells. HEK293T cells were transfected with a plasmid expressing the circular Corn-SAM sensor. 3 d after transfection, cells were treated with 25 mM cycloleucine for 1 h. Total cellular RNA was harvested by using TRIzol LS. Cellular RNA (1.5 µg) was loaded in each lane of a 6% TBE-Urea PAGE gel. After PAGE, the gel was washed three times for 5 min each with water to remove urea from the gel. Then, the gel was first stained with 10 µM DFHO and 0.1 mM SAM (left), followed by a counterstaining with SYBR Gold (right). The DFHO stained gel was imaged using a ChemiDoc Imaging station (BioRad) at the green channel (excitation 470/30 nm; emission 530/28 nm) and red channel (excitation 530/28 nm; emission 605/50 nm). The image shown here is the overlay of both scans. The SYBR Gold stained gel was imaged using standard imaging settings (excitation 302 nm; emission 590/110 nm).

Red dotted boxes indicate circular Corn-SAM sensor RNA. Three replicates are shown on the gel images. No overall change in total Corn-SAM sensor RNA levels was detected after the cycloleucine addition in any of the replicates.

(C) Denaturing PAGE analysis of whole cellular RNA harvested from cells transfected with different amount of the Corn-SAM sensor-expressing plasmid. HEK293T cells were transfected with 250 ng, 500 ng (the amount used elsewhere throughout this study) or 1000 ng of a plasmid expressing the circular Corn-SAM sensor. 3.5 d after transfection, total cellular RNA was harvested by using TRIzol LS. Cellular RNA (1.5 µg) was resolved on 6% TBE-Urea PAGE gel and stained as described in panel B.

Red dotted boxes indicate circular Corn-SAM sensor RNA. Higher level of circular Corn-SAM sensor RNA was detected when a larger amount of a plasmid was transfected.

(D) To test the effect of Corn-SAM sensor RNA concentration in cells, HEK293T cells were transfected with 250 ng, 500 ng, 1000 ng of a plasmid expressing the circular Corn-SAM sensor as described in panel C. 3.5 d after transfection, we imaged cells for 1 h after addition of 25 mM cycloleucine. Cellular mean fluorescence intensity was calculated (See **Methods**), and normalized to maximum intensity at time 0 (100) and background intensity (0). The average values of mean fluorescence intensity calculated from n = 8 cells (from 5 fields of view) were plotted as dots against time. Error bars indicate SEM values.

In cells expressing the highest levels of the Corn-SAM sensor RNA, the rate of fluorescence loss after cycloleucine treatment was slower compared to cells expressing the lowest levels of

sensor RNA (time to half-maximal fluorescence was increased by ~6 min). Thus, the expression levels should be consistent in different experiments when comparing rates of fluorescence change using this sensor.

(E) Single-cell imaging of the circular Corn-SAM sensor fluorescence in response to cycloleucine and actinomycin D treatment. HEK293T cells were transfected with plasmids expressing the circular Corn-SAM sensor. After 4 d, we imaged cells for 1 h after addition of 25 mM cycloleucine and 5 μg/mL actinomycin D. As a control, cells were incubated with 25 mM cycloleucine only. Images were acquired using a 40× air objective (NA 0.75) and YFP filter cube (ex 500 ± 12 nm; em 542 ± 13.5 nm). Acquisition time 500 ms. Scale bar 10 μm.

(F) SAM trajectory plots of 5 individual cells for each condition selected from 2 biological replicates. Each trajectory plot was generated based on the mean fluorescence intensity in single cells during the time-course imaging experiment. In case of each cell, mean fluorescence intensities were calculated at 13 time points over a 1 h imaging experiment (See **Methods**). Actinomycin D did not induce any noticeable change in the decrease rates of Corn-SAM sensor signal.

Table S1, related to Figures 4A and S3C. Full length RNA sequences of the linear Corn-SAM sensor, the nascent transcript of the circular Corn-SAM sensor before processing for circularization and the circular Corn-SAM sensor.

	Sequence
Linear Corn-SAM sensor (126 nt)	5'- GUGCUCGCUUCGGCAGCACAUAUACUAGUCGACCGCCAGA UGCCUUGUAACCGAAAGGGUGAGGAAGGAGGUCUGAGGAG GUCACUACGAAAGGAUGGCGUCUAGAGCGGACUUCGGTCC GCUUUU -3'
Circular Corn-SAM sensor nascent transcript (285 nt)	5'- GUGCUCGCUUCGGCAGCACAUAUACUAGUCGACGGGCCGC ACUCGCCGGTCCCAAGCCCGGAUAAAAUGGGAGGGGGCGG GAAACCGCCUAACCAUGCCGAGTGCGGCCGCCGCCAGAUG CCUUGUAACCGAAAGGGUGAGGAAGGAGGUCUGAGGAGGU CACUACGAAAGGAUGGCGGUGGCCGCGGUCGGCGUGGAC UGUAGAACACUGCCAAUGCCGGUCCCAAGCCCGGAUAAAA GUGGAGGGUACAGUCCACGCUCUAGAGCGGACUUCGGUC CGCUUUU -3'
Circular Corn-SAM sensor after self-cleavage (114 nt)	5'- AACCAUGCCGAGTGCGGCCGCCGCCAGAUGCCUUGUAACC GAAAGGGUGAGGAAGGAGGUCUGAGGAGGUCACUACGAAA GGAUGGCGGUGGCCGCGGUCGGCGUGGACUGUAG -3'
Circular Corn-SAM sensor after ligation	AACCAUGCCGAGTGCGGCCGCCGCCAGAUGCCUUGUAACC GAAAGGGUGAGGAAGGAGGUCUGAGGAGGUCACUACGAAA GGAUGGCGGUGGCCGCGGUCGGCGUGGACUGUAG

Table S2, related to Figures 1, 2, 3, S1, S2, S3A and S3B. DNA primers to prepare dsDNA templates for *in vitro* transcription.

	Sequence (5' → 3')

Forward primer_Broccoli fused to circularly permuted SAM aptamer	CCAT**TAATACGACTCACTATAGGG**CGCCAGATGCCTTGTAACCGAAAGGGTGTCGA
ssDNA template_ Broccoli fused to circularly permuted SAM aptamer	GTAACCGAAAGGGTGTCGAGTAGAGTGTGGGCTCCTGCCATCAGTCGGCTTCGGCCGA
Reverse primer_ Broccoli fused to circularly permuted SAM aptamer	CGCCATCCTTTCGTGGACCCGACCGTCTCCTGCCATCAGTCGGCCGAAGCCG
Forward primer_Broccoli	CCAT**TAATACGACTCACTATAGGG**CGGCCGCGAGACGGTCGGG
Reverse primer_Broccoli	GCGGCCACGAGCCCACACTCTACTCGACAGATACGAATATCTGGACCCGACCGTCTCGCG
Forward primer_Corn-SAM sensor (Transducer 1)	CCAT**TAATACGACTCACTATAGGG**CGCCAGATGCCTTGTAACCGAAAGGG
Reverse primer_Corn-SAM sensor (Transducer 1)	CGCCATCCTTTCGTCAGTGACCTCCTCAGACCTCCTTCCTCGACCCTTTCGGTTACAAGG
Forward primer_Corn-SAM sensor (Transducer 2)	CCAT**TAATACGACTCACTATAGGG**CGCCAGATGCCTTGTAACCGAAAGGG
Reverse primer_Corn-SAM sensor (Transducer 2)	CGCCATCCTTTCGTAGTGACCTCCTCAGACCTCCTTCCTCACCCTTTCGGTTACAAGGC
Forward primer_Corn-SAM sensor (Transducer 3)	CCAT**TAATACGACTCACTATAGGG**CGCCAGATGCCTTGTAACCGAAAGGGCT
Reverse primer_Corn-SAM sensor (Transducer 3)	CGCCATCCTTTCGCTAGTGACCTCCTCAGACCTCCTTCCTCAGCCCTTTCGGTTACA
Forward primer_Corn-SAM sensor (Transducer 4)	CCAT**TAATACGACTCACTATAGGG**CGCCAGATGCCTTGTAACCGAAAGGGCT
Reverse primer_Corn-SAM sensor (Transducer 4)	CGCCATCCTTTCGCTTAGTGACCTCCTCAGACCTCCTTCCTCAAGCCCTTTCGGTTACA
Forward primer_Corn-SAM sensor (Transducer 5)	CCAT**TAATACGACTCACTATAGGG**CGCCAGATGCCTTGTAACCGAAAGGG
Reverse primer_Corn-SAM sensor (Transducer 5) (Figure 1D)	CGCCATCCTTTCGGGAAAGTGACCTCCTCAGACCTCCTTCCTCTTCCCCCTTTCGGTTACAAGGC
Forward primer_Corn-SAM sensor (Transducer 6) (Figure 1D)	CCAT**TAATACGACTCACTATAGGG**CGCCAGATGCCTTGTAACCGAAAGGG
Reverse primer_Corn-SAM sensor (Transducer 6)	CGCCATCCTTTCGGTTTAGTGACCTCCTCAGACCTCCTTCCTCAAACCCCTTTCGGTTACAAGGC
Forward primer_Corn-SAM sensor (Transducer 7)	CCAT**TAATACGACTCACTATAGGG**CGCCAGATGCCTTGTAACCGAAAGGG
Reverse primer_Corn-SAM sensor (Transducer 7)	CGCCATCCTTTCGTTGTAGTGACCTCCTCAGACCTCCTTCCTCAACACCCTTTCGGTTACAAGGC
Forward primer_Corn-SAM sensor (Transducer 8)	CCAT**TAATACGACTCACTATAGGG**CGCCAGATGCCTTGTAACCGAAAGGG
Reverse primer_Corn-SAM sensor (Transducer 8)	CGCCATCCTTTCGAGGAAAGTGACCTCCTCAGACCTCCTTCCTCTTCCTCCCTTTCGGTTACAAGGC
Forward primer_Corn-SAM sensor (Transducer 9)	CCAT**TAATACGACTCACTATAGGG**CGCCAGATGCCTTGTAACCGAAAGGG

Reverse primer_Corn-SAM sensor (Transducer 9)	CGCCATCCTTTCGAAGGAAAGTGACCTCCTCAGACCT CCTTCCTCTTCCTTCCCTTTCGGTTACAAGGC
Forward primer_Corn-cdiGMP sensor_2nd round PCR	CCAT**TAATACGACTCACTATAGGG**TGGTAGGTAGCGG GGTTAC
Reverse primer_Corn-cdiGMP sensor_2nd round PCR	TGGTTTAGGCCGGAGGCTTTGCGTCCCACTCTTTCGA ATGGTTTGCCCTGTG
Forward primer_Corn-cdiGMP sensor (Transducer 1)_1st round PCR	GTGGTAGGTAGCGGGGTTACGGAAGAGGAAGGAGGT CTGAGGAGGTCACT
Reverse primer_Corn-cdiGMP sensor (Transducer 1)_1st round PCR	TCGAATGGTTTGCCCTGTGGGAAAGTGACCTCCTCAG ACCTCC
Forward primer_Corn-cdiGMP sensor (Transducer 2)_1st round PCR	GTGGTAGGTAGCGGGGTTACCGATGGAGGAAGGAGG TCTGAGGAGGTCACT
Reverse primer_Corn-cdiGMP sensor (Transducer 2)_1st round PCR	TCGAATGGTTTGCCCTGTGCGTGAGTGACCTCCTCAG ACCTCC
Forward primer_Corn-cdiGMP sensor (Transducer 3)_1st round PCR	GTGGTAGGTAGCGGGGTTACCGATTGAGGAAGGAGGT CTGAGGAGGTCACT
Reverse primer_Corn-cdiGMP sensor (Transducer 3)_1st round PCR	TCGAATGGTTTGCCCTGTGCGTTAGTGACCTCCTCAGA CCTCC
Forward primer_Corn-cdiGMP sensor (Transducer 4)_1st round PCR	GTGGTAGGTAGCGGGGTTACCGAGTGAGGAAGGAGG TCTGAGGAGGTCACT
Forward primer_Corn-cdiGMP sensor (Transducer 4)_1st round PCR	TCGAATGGTTTGCCCTGTGCGGTAGTGACCTCCTCAG ACCTCC
Forward primer_Corn-SAH sensor_2nd round PCR	CCAT**TAATACGACTCACTATAGGG**CTCGCCGAGGAGC GCTGCAA
Reverse primer_Corn-SAH sensor_2nd round PCR	CTGAACCGAGCGCCG
Forward primer_Corn-SAH sensor (Transducer 1)_1st round PCR	CCGAGGAGCGCTGCAACAGGAAGAGGAAGGAGGTCT GAGGAGGTCACTTTCCTGCCAGGC
Reverse primer_Corn-SAH sensor (Transducer 1)_1st round PCR	CTGAACCGAGCGCCGTTGGTTTAAAGGTCCCGATAAT CGCCGAGCCTGGCAGGAAAGTGA
Forward primer_Corn-SAH sensor (Transducer 2)_1st round PCR	CGAGGAGCGCTGCAAAGGAAGAGGAAGGAGGTCTGA GGAGGTCACTTTCCTCCAGGCTCG
Reverse primer_Corn-SAH sensor (Transducer 2)_1st round PCR	CTGAACCGAGCGCCGTTGGTTTAAAGGTCCCGATAAT CGCCGAGCCTGGAGGAAAGTGAC
Forward primer_Corn-SAH sensor (Transducer 3)_1st round PCR	CCGAGGAGCGCTGCAAGGAAGAGGAAGGAGGTCTGA GGAGGTCACTTTCCCCAGGCTCGG

Reverse primer_Corn-SAH sensor (Transducer 3)_1st round PCR	CTGAACCGAGCGCCGTTGGTTTAAAGGTCCCGATAATCGCCGAGCCTGGGGAAAGTG
Forward primer_Corn-SAH sensor (Transducer 4)_1st round PCR	CCGAGGAGCGCTGCAACGGAAGAGGAAGGAGGTCTGAGGAGGTCACTTTCCGCCAGGCTC
Reverse primer_Corn-SAH sensor (Transducer 4)_1st round PCR	CTGAACCGAGCGCCGTTGGTTTAAAGGTCCCGATAATCGCCGAGCCTGGCGGAAAGTGAC
Forward primer_Corn-SAH sensor (Transducer 5)_1st round PCR	CCGAGGAGCGCTGCAAGGTAAGAGGAAGGAGGTCTGAGGAGGTCACTTTACCCCAGGCTC
Reverse primer_Corn-SAH sensor (Transducer 5)_1st round PCR	TGAACCGAGCGCCGTTGGTTTAAAGGTCCCGATAATCGCCGAGCCTGGGGTAAAGTGACC
Forward primer_tRNA-Corn	CCAT**TAATACGACTCACTATAGGG**GCCCGGATAGCTCAGTCGGTAGAGCAGCGGCCG
tRNA-Corn template from pAV-tCorn (Song et al., 2017)	GAGCAGCGGCCGCGAGGAAGGAGGTCTGAGGAGGTCACTGCGGCCGCGGGTCCAG
Reverse primer_tRNA-Corn	TGGCGCCCGAACAGGGACTTGAACCCTGGACCCGCGGC

*The bold DNA sequences indicate the T7 promoter region.

Table S3, related to Figures 4, S3 and S4. DNA primers to prepare dsDNA templates for cloning.

	Sequence (5' → 3')
Forward primer_Corn-SAM sensor in pAV-Tornado-Corn-SAM sensor	AATCAT*GCGGCCGC*CGCCAGATGCCTTGTAACCG
Reverse primer_Corn-SAM sensor in pAV-Tornado-Corn-SAM sensor	GTAATT*CCGCGG*CCACCGCCATCCTTTCGGGAAAGTG
Forward primer_Corn-SAM sensor in pAV-Corn-SAM sensor	AATCTA*GTCGAC*CGCCAGATGCCTTGTAACC
Reverse primer_Corn-SAM sensor in pAV-Corn-SAM sensor	AACAAT*TCTAGA*CGCCATCCTTTCGG
DNA Template_Corn SAM sensor	CGCCAGATGCCTTGTAACCGAAAGGGGGAAGAGGAAGGAGGTCTGAGGAGGTCACTTTCCCGAAAGGATGGCG

*DNA sequences in italic and underlined indicate restriction enzyme sites.